Research Article | Vol. 7, No. 12 | 1 Dec 2016 | BIOMEDICAL OPTICS EXPRESS 5208

Biomedical Optics EXPRESS

Ultrafast time-stretch imaging at 932 nm through a new highly-dispersive fiber

XIAOMING WEI,[1] CIHANG KONG,[1] SAMUEL SY,[2] HO KO,[3,4,5] KEVIN K. TSIA,[1] AND KENNETH K. Y. WONG[1,*]

[1]*Department of Electrical and Electronic Engineering, The University of Hong Kong, Pokfulam Road, Hong Kong, China*
[2]*Department of Electronic Engineering, Faculty of Engineering, The Chinese University of Hong Kong, Hong Kong, China*
[3]*Department of Medicine and Therapeutics, Prince of Wales Hospital, Faculty of Medicine, Chinese University of Hong Kong, Hong Kong, China*
[4]*Li Ka Shing Institute of Health Sciences, Faculty of Medicine, The Chinese University of Hong Kong, Hong Kong, China*
[5]*ho.ko@alumni.ucl.ac.uk*
[*]*kywong@eee.hku.hk*

Abstract: Optical glass fiber has played a key role in the development of modern optical communication and attracted the biotechnology researcher's great attention because of its properties, such as the wide bandwidth, low attenuation and superior flexibility. For ultrafast optical imaging, particularly, it has been utilized to perform MHz time-stretch imaging with diffraction-limited resolutions, which is also known as serial time-encoded amplified microscopy (STEAM). Unfortunately, time-stretch imaging with dispersive fibers has so far mostly been demonstrated at the optical communication window of 1.5 μm due to lack of efficient dispersive optical fibers operating at the shorter wavelengths, particularly at the bio-favorable window, i.e., <1.0 μm. Through fiber-optic engineering, here we demonstrate a 7.6-MHz dual-color time-stretch optical imaging at bio-favorable wavelengths of 932 nm and 466 nm. The sensitivity at such a high speed is experimentally identified in a slow data-streaming manner. To the best of our knowledge, this is the first time that all-optical time-stretch imaging at ultrahigh speed, high sensitivity and high chirping rate (>1 ns/nm) has been demonstrated at a bio-favorable wavelength window through fiber-optic engineering.

OCIS codes: (060.2350) Fiber optics imaging; (060.3510) Lasers, fiber; (060.2280) Fiber design and fabrication; (300.6530) Spectroscopy, ultrafast; (170.7160) Ultrafast technology.

References and links

1. E. R. Andresen, C. K. Nielsen, J. Thøgersen, and S. R. Keiding, "Fiber laser-based light source for coherent anti-Stokes Raman scattering microspectroscopy," Opt. Express **15**(8), 4848–4856 (2007).
2. C. W. Freudiger, W. Yang, G. R. Holtom, N. Peyghambarian, X. S. Xie, and K. Q. Kieu, "Stimulated Raman scattering microscopy with a robust fibre laser source," Nat. Photonics **8**(2), 153–159 (2014).
3. N. G. Horton, K. Wang, D. Kobat, C. G. Clark, F. W. Wise, C. B. Schaffer, and C. Xu, "In vivo three-photon microscopy of subcortical structures within an intact mouse brain," Nat. Photonics **7**(3), 205–209 (2013).
4. R. Huber, M. Wojtkowski, and J. G. Fujimoto, "Fourier Domain Mode Locking (FDML): A new laser operating regime and applications for optical coherence tomography," Opt. Express **14**(8), 3225–3237 (2006).
5. A. M. Zysk, F. T. Nguyen, A. L. Oldenburg, D. L. Marks, and S. A. Boppart, "Optical coherence tomography: a review of clinical development from bench to bedside," J. Biomed. Opt. **12**(5), 051403 (2007).
6. K. Goda, K. K. Tsia, and B. Jalali, "Serial time-encoded amplified imaging for real-time observation of fast dynamic phenomena," Nature **458**(7242), 1145–1149 (2009).
7. K. Goda, D. R. Solli, K. K. Tsia, and B. Jalali, "Theory of amplified dispersive Fourier transformation," Phys. Rev. A **80**(4), 043821 (2009).
8. B. Jalali, J. Chan, and M. H. Asghari, "Time–bandwidth engineering," Optica **1**(1), 23–31 (2014).
9. K. K. Tsia, K. Goda, D. Capewell, and B. Jalali, "Performance of serial time-encoded amplified microscope," Opt. Express **18**(10), 10016–10028 (2010).
10. J. P. Clifford, G. Konstantatos, K. W. Johnston, S. Hoogland, L. Levina, and E. H. Sargent, "Fast, sensitive and spectrally tuneable colloidal-quantum-dot photodetectors," Nat. Nanotechnol. **4**(1), 40–44 (2009).

#278224 http://dx.doi.org/10.1364/BOE.7.005208
Journal © 2016 Received 6 Oct 2016; revised 12 Nov 2016; accepted 12 Nov 2016; published 18 Nov 2016

Biomedical Optics EXPRESS

11. V. J. Matsas, T. P. Newson, D. J. Richardson, and D. N. Payne, "Selfstarting passively mode-locked fibre ring soliton laser exploiting nonlinear polarisation rotation," Electron. Lett. **28**(24), 2226–2228 (1992).
12. X. Wei, J. Xu, Y. Xu, L. Yu, J. Xu, B. Li, A. K. S. Lau, X. Wang, C. Zhang, K. K. Tsia, and K. K. Y. Wong, "Breathing laser as an inertia-free swept source for high-quality ultrafast optical bioimaging," Opt. Lett. **39**(23), 6593–6596 (2014).
13. C. Bartolacci, M. Laroche, H. Gilles, S. Girard, T. Robin, and B. Cadier, "Generation of picosecond blue light pulses at 464 nm by frequency doubling an Nd-doped fiber based Master Oscillator Power Amplifier," Opt. Express **18**(5), 5100–5105 (2010).
14. M. Laroche, B. Cadier, H. Gilles, S. Girard, L. Lablonde, and T. Robin, "20 W continuous-wave cladding-pumped Nd-doped fiber laser at 910 nm," Opt. Lett. **38**(16), 3065–3067 (2013).
15. K. Qian, H. Wang, M. Laroche, and A. Hideur, "Mode-locked Nd-doped fiber laser at 930 nm," Opt. Lett. **39**(2), 267–270 (2014).
16. X. Gao, W. Zong, B. Chen, J. Zhang, C. Li, Y. Liu, A. Wang, Y. Song, and Z. Zhang, "Core-pumped femtosecond Nd:fiber laser at 910 and 935 nm," Opt. Lett. **39**(15), 4404–4407 (2014).
17. B. Chen, T. Jiang, W. Zong, L. Chen, Z. Zhang, and A. Wang, "910nm femtosecond Nd-doped fiber laser for in vivo two-photon microscopic imaging," Opt. Express **24**(15), 16544–16549 (2016).
18. A. Wetter, M. Faucher, and B. Sevigny, "High power cladding light strippers," Proc. SPIE **6873**, 687327 (2008).
19. A. Chong, J. Buckley, W. Renninger, and F. Wise, "All-normal-dispersion femtosecond fiber laser," Opt. Express **14**(21), 10095–10100 (2006).
20. http://www.teraxion.com/
21. D. J. Beebe, J. S. Moore, J. M. Bauer, Q. Yu, R. H. Liu, C. Devadoss, and B. H. Jo, "Functional hydrogel structures for autonomous flow control inside microfluidic channels," Nature **404**(6778), 588–590 (2000).
22. B. Chung, H. Ng, M. Wang, S. C. V. Bogaraju, A. H. C. Shum, H. K. H. So, and K. K. Tsia, "High-throughput microparticle screening by 1-μm time-stretch optofluidic imaging integrated with a field-programmable gate array platform," in Conference on Lasers and Electro-Optics, OSA Technical Digest (2016) (Optical Society of America, 2016), paper STh3G.4.
23. K. Goda, A. Ayazi, D. R. Gossett, J. Sadasivam, C. K. Lonappan, E. Sollier, A. M. Fard, S. C. Hur, J. Adam, C. Murray, C. Wang, N. Brackbill, D. Di Carlo, and B. Jalali, "High-throughput single-microparticle imaging flow analyzer," Proc. Natl. Acad. Sci. U.S.A. **109**(29), 11630–11635 (2012).
24. T. T. W. Wong, A. K. S. Lau, K. K. Y. Ho, M. Y. H. Tang, J. D. F. Robles, X. Wei, A. C. S. Chan, A. H. L. Tang, E. Y. Lam, K. K. Y. Wong, G. C. F. Chan, H. C. Shum, and K. K. Tsia, "Asymmetric-detection time-stretch optical microscopy (ATOM) for ultrafast high-contrast cellular imaging in flow," Sci. Rep. **4**, 3656 (2014).

1. Introduction

Although it has become increasingly popular in recent years, extra efforts are needed to improve the reliability, portability and cost-efficiency of those bio-optical systems for their practically clinical applications. This is particularly the case for optical bio-imaging systems involving bulky and expensive laser sources, e.g., the Ti:sapphire lasers, which more or less hinder the worldwide applications beyond laboratories. Optical fiber, as the backbone of the modern optical communication, has drawn intensive attention from the bio-imaging research for its ultra-wide bandwidth, low attenuation and superior flexibility. It has been widely perceived as an alternative to expensive and bulky solid-state lasers. Pioneer efforts include coherent anti-Stokes Raman scattering (CARS) imaging [1], stimulated Raman scattering (SRS) microscopy [2], multiphoton brain imaging [3], and optical coherence tomography (OCT) [4], to name a few. Particularly, OCT has enabled a wide range of clinical applications due to its compact design and low cost [5].

Nevertheless, the speed of those optical imaging systems mentioned before, typically in the vicinity of a video rate, is limited by two main factors: firstly, the raster scanning usually required for the 2D/3D imaging, is a time-consuming approach, particularly when the mechanical motion is involved; secondly, it takes a long integration time to collect the optical signal for a moderate signal-to-noise ratio (SNR). As a consequence, ultrafast diagnosis involving transient processes is largely hindered. All-optical time-stretch microscopy [6] is an emerging ultrafast optical imaging modality that can provide an unprecedented imaging speed with a line-scan rate up to 10's of MHz. The magic behind the time-stretch technology is the wavelength-to-time mapping inherited from optical dispersive elements [7], e.g., dispersion-compensating fiber (DCF) [6]. The temporal spectrum, which is encoded with the spatial information through the wavelength-to-time mapping, can be efficiently captured in a single-shot manner and then reconstructed into 2D images through off-line data processing. In spite

Biomedical Optics EXPRESS

of the ultrahigh throughput capacity, it is also a high-data-streaming imaging modality — easily >50 GS/s [6], which is even beyond the processing capability of the state-of-the-art electrical signal processors [8]. As a consequence, a large electrical bandwidth, typically >10 GHz, is usually required to fully interpret the spectral information [9]. This can exert excessive pressure on the optical detectors and results in difficulties in manipulating the trade-off between bandwidth and sensitivity [10]. A larger dispersion (i.e., a higher chirping rate), provided by a more transparent dispersive medium, cannot only reduce the electrical bandwidth and thus enhance the detection sensitivity, but also decrease the effective data amount for interpreting spectral information. Unfortunately, such a high figure-of-merit dispersive fiber has not yet been exploited at the bio-favorable wavelength window (typically 400-1000 nm), which is also the reason why most of previous works have been demonstrated at the telecommunication window [6,7].

Here, we demonstrate a sensitive time-stretch imaging at the bio-favorable windows from 932 nm to 466 nm through fiber-optic engineering. By introducing a highly-dispersive fiber (HDF), which is particularly designed for a wavelength range of 800-1100 nm, a dispersion of >1.6 ns/nm is obtained with a much better transparency. Based on this, we design an ultrafast all-optical swept source at 932 nm with a special W-type gain fiber. To the best of our knowledge, this has not yet been demonstrated. It is then applied to a modified spectrally-encoded microscopy to perform MHz time-stretch optical imaging at a much slower data rate, i.e., <5 GS/s, which is almost 10 times slower than that of previous works at 1.5 μm [6]. In the meantime, a better spatial resolution can potentially be obtained, which is naturally inherited from a shorter wavelength. It is the first time that MHz bio-imaging at the biological window is realized with fiber laser source. In addition, we also propose and demonstrate ultrafast optical imaging simultaneously at 466 nm, where the lowest bio-absorption is expected. We believe that our results can enable real-time high throughput optical imaging at visible window in a lower data-streaming manner.

2. The swept source at 932 nm (SS@932nm)

The configuration of the ultrafast fiber-based swept source at 932 nm is illustrated in Fig. 1. It includes three key parts: short-pulse generation, wavelength sweeping and power booster, as labeled in Fig. 1. For the short pulse generation, nonlinear polarization rotation (NPR) mode-locking was introduced to a fiber ring resonator [11,12]. The gain medium was a 20-m double-cladding neodymium-doped fiber (NDF), iXblue IXF-2CF-Nd 5-125 [13–15]. The NDF has a core size of 5 ± 0.5 μm and a standard cladding diameter of 125 ± 3 μm. Its core numerical aperture (NA, ~0.14) has been designed to match with the standard single-mode fiber (SMF), e.g., the Nufern 1060-xp and Corning HI 1060. Typically, NDF exhibits a strong emission at around 1060 nm, and thus the NDF cavity easily oscillates at 1060 nm rather than 900 nm [16,17]. The NDF used here has a W-type refractive index profile, and more detailed information can be found iXblue. It generates an effective cutoff wavelength of <950 nm for the LP_{01} mode, i.e., the fundamental transverse mode. In this design, the propagation of LP_{01} mode exhibits a larger attenuation for longer wavelengths, and thus effectively suppresses the emission of 1060 nm [15], which is evident by the amplified spontaneous emission (ASE) optical spectra shown in Fig. 2(a). Furthermore, the bending loss of optical fiber is spectrally sensitive to the bending radius, i.e., a longer wavelength has a higher bending loss for a smaller bending radius. Consequently, the W-type NDF can work together with bending loss to perform spectral filtering. Figure 2(b) shows the wavelength shifting by changing the coiling diameter of NDF. It is clear that the operating center wavelength can be gradually blue-shifted with a decreasing coiling diameter.

Biomedical Optics EXPRESS

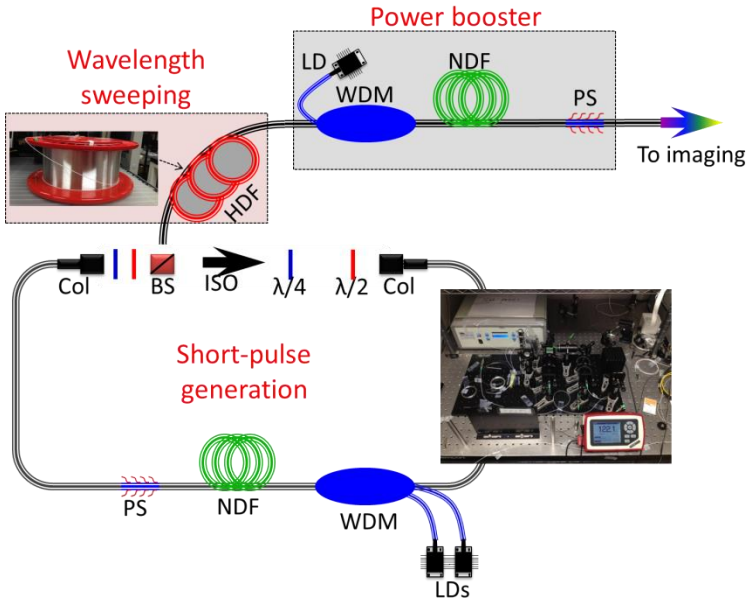

Fig. 1. The schematic diagram of the MHz fiber-based swept source at 932 nm. The insets are the photos of the new HDF and the actual setup of the swept source built on a 30 × 60 cm aluminum breadboard. NDF: neodymium-doped fiber; LD: laser diode; WDM: wavelength-division multiplexing; Col: collimator; BS: beam splitter; ISO: isolator; λ/2: half-wave plate; λ/4: quarter-wave plate; PS: pump stripper.

The pump laser was a custom-made three-in-one fiber-pigtailed laser diode (LD) box. Each LD with 105/125-μm multimode fiber (MMF) can deliver a maximum power of ~3.5 W at 808 nm. Two of them were combined through a 1 + 2 signal/pump wavelength-division multiplexing (WDM) to pump the gain fiber. The fiber pigtails of the WDM have been optimized to match with the NA and core size of the rest fibers in the fiber cavity, e.g., 6/125-μm double-cladding fiber (Coractive DCF-UN-6/125-14, NA = 0.14) for both signal and common ports, while 105/125-μm MMF (Nufern MM-S105/125-0.22NA, NA = 0.22) for the pump ports. It should be pointed out that the pump absorption of current gain fiber is relatively low, only ~0.15 dB/m. It implies that part of the pump power cannot be absorbed by the gain fiber. Thus, the residual pump power should be extracted from the fiber resonator; otherwise, the splicing point between the gain fiber and passive SMF can be easily burned since most of the residual pump power can be consumed at the splicing point to heat up the SMF. Here, a simple approach was employed to break the guiding property of the double-cladding fiber by using polymer material with a high refractive index [18], i.e., a UV-curable polymer with a refractive index of 1.56 (Thorlabs NOA63) was used to recoat the splicing area. The recoating length should be long enough to gradually extract the residual pump power, i.e., ~3 cm in this case. The recoating area was then adhered on a grooved aluminum plate for cooling.

Biomedical Optics EXPRESS

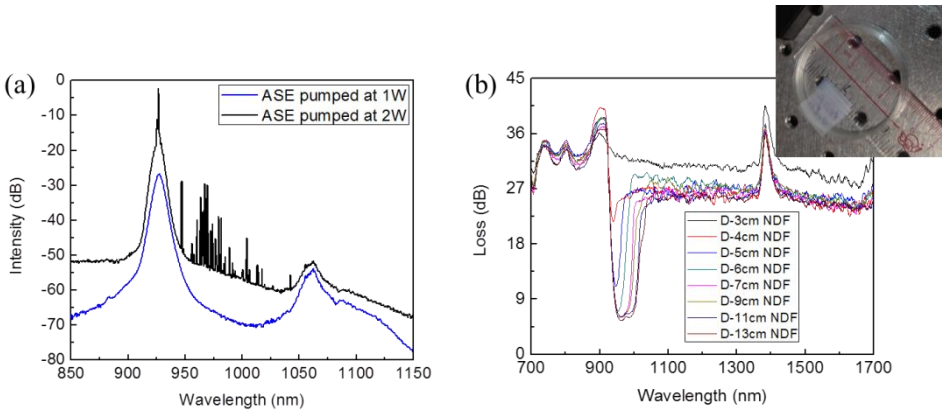

Fig. 2. (a) The ASE spectra of the W-type NDF pumped at different power levels. It should be pointed out that no cavity was constructed in this measurement. (b) The loss characteristic of the W-type NDF with different coiling diameters. Inset shows a coiled NDF with a diameter of 5 cm.

The amplified signal from NDF was then launched into the free space through a fiber collimator (Col, Thorlabs F220APC-980) for the polarization control and signal extraction. A 30:70 beam splitter (BS) was used to extract 70% of the optical signal from the fiber resonator, while 30% of the signal was coupled back to the fiber cavity via another fiber collimator for oscillation. The NPR mode-locking was realized by the combination of half-/quarter-wave plates (λ/2 and λ/4, Thorlabs WPH05M-980 and WPQ05M-980) and polarization-dependent isolator (ISO, Thorlabs IO-5-980-VLP), which simultaneously provides a polarization-sensitive loss and unidirectional operation. In general, self-started mode-locking in such a fiber cavity cannot be obtained owing to the all-normal dispersion issue, and usually an extra bandpass filter is required to overcome this problem [19]. In this work, however, the bandpass filtering effect can be attained from its narrow gain bandwidth and loss characteristic of the gain fiber, as shown in Figs. 2(a) and 2(b), respectively.

To perform all-optical wavelength sweeping, the short pulse output from the fiber cavity went through a new HDF, which was custom-made from OFS (model No., DCF solution for 800-1100 nm). In principle, the dispersive medium used for all-optical time-stretch should not only have a high chirping rate but also a low attenuation. Indeed, such a dispersive fiber can be easily found at the optical communication wavelength window of 1.3-1.5 μm, and a dispersion-to-loss ratio (DLR) of >150 ps/nm per dB can be obtained from the SMF-based dispersion-compensating modules, e.g., Corning DCM-100-SMF-C and Lucent DSCM. However, such dispersive fibers are not existed at the shorter wavelength. In addition, those commonly-used SMFs at the shorter wavelength window exhibit a very low DLR, typically <20 ps/nm per dB, e.g., Nufern 1060-xp and Corning HI 1060. It is almost 8 times worse than that of the telecommunication DCFs. Although chirped fiber Bragg gratings (FBGs) can provide a better performance in term of the dispersion coefficient, their bandwidth is typically limited to sub-nm at a high chirping rate [20]. The new HDF introduced here can overcome those limitations. The DLR of the new HDF was measured to be ~100 ps/nm per dB at 1060 nm, which is five times better than that of the existing SMFs at this window [24], as shown in Fig. 3(a). The loss during the wavelength sweeping process was then compensated by an external optical fiber amplifier, which composes of another 10-m NDF, a WDM and a pump LD. After the gain fiber, another residual pump stripper was employed to extract the residual pump power. An average optical power of ~18 dBm at 932 nm was obtained after the external amplifier. The wavelength-swept pulse waveform is illustrated in Fig. 3(b). As can be observed, the period of the wavelength sweeping is 131 ns, yielding a frame rate of 7.6 MHz. The linear mapping from spectral to temporal domains was also evaluated and an acceptable

Biomedical Optics EXPRESS

performance was achieved, as shown in Fig. 3(c). It is clear that the wavelength scans over 7.2 nm within 8.4 ns, yielding a sweeping speed of ~860000000 nm/s. The wavelength-swept pulse at 932 nm was finally launched into the free-space optical system for ultrafast optical imaging.

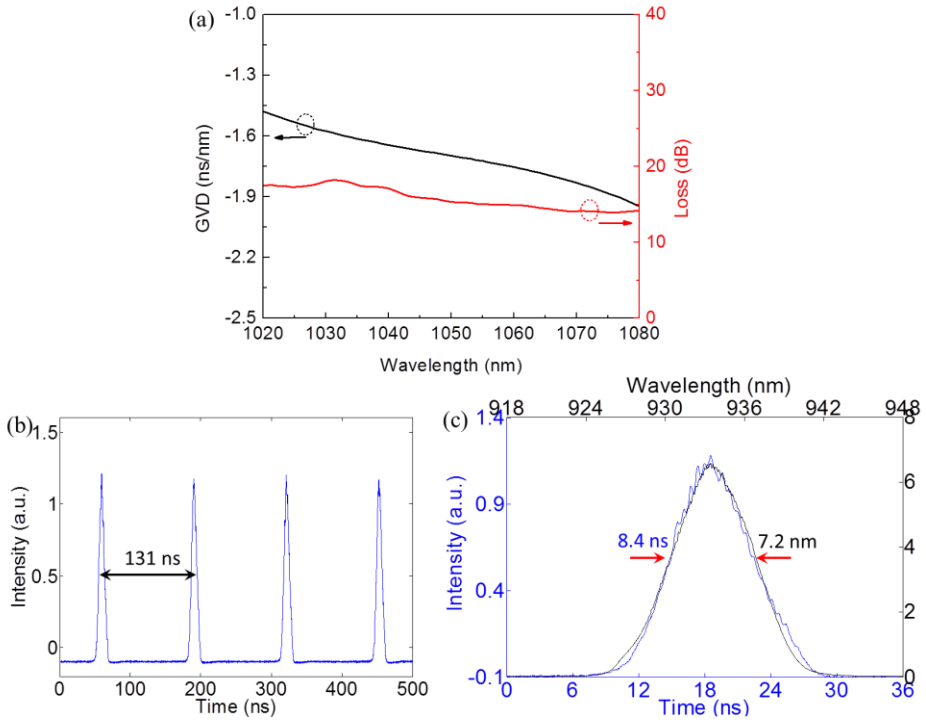

Fig. 3. (a) The dispersion and loss properties of the new highly-dispersive fiber. It should be pointed out that the measurement was limited by the wavelength tunability of laser source. (b) The wavelength-swept pulse waveform train captured by a real-time oscilloscope. (c) The single-shot temporal optical spectrum and the averaged optical spectrum measured by a conventional optical spectrum analyzer (OSA).

3. Dual-color time-stretch imaging

Figure 4 shows the overall configuration of the ultrafast dual-color time-stretch imaging system. The wavelength-swept pulse at 932 nm (denoted as SS@932nm) was spatially dispersed by a reflective diffraction grating with a groove density of 600/mm, Thorlabs GR25-0610. After the grating, the laser beam was imprinted with wavelength-dependent angular dispersion, resulting in a 1D spectral array. The spectral array was then relayed to the objective lens OL1 through an optical telescope (L1 and L2). To simultaneously perform dual-color imaging at both visible and near-infrared (NIR) windows, a nonlinear BBO crystal was placed at the Fourier plane of L1 for second-harmonic generation (SHG). Since the fundamental beam cannot be completely annihilated for the new photon generation, dual spectral arrays at both 932 nm and 466 nm were co-existed after the nonlinear crystal. Thus, the spatial information of the sample can be encoded into both 1D spectral arrays after the optical illuminations. After the optical illumination, the laser beams were collected by an identical objective lens (OL2) and then relayed by another optical telescope (L3 and L4) to an identical diffraction grating for angular dispersion stripping. Finally, the wavelength-swept pulse waveforms at different wavelengths were separated by a dichroic mirror (DM) and detected by the photodiodes (PDs), as shown in Fig. 4. Indeed, extra free-space filters can be employed to select either spectral array, e.g., 785-nm shortpass filter (Semrock BSP01-785R-

Biomedical Optics EXPRESS

25) for the 466-nm spectral array and 785-nm longpass filter (Semrock BLP01-785R-25) for the 932-nm one, respectively. To obtain 2D images, extra 1D scanning perpendicular to that of the spectral array is required. Subject to different samples under inspection, specific schemes can be utilized, e.g., microfluidic flow channel for cellular samples [21] and optical beam scanning via high-speed acousto-optic deflector (AOD) or galvanometer mirror for static tissue samples. In this work, we temporally used a translation stage together with an actuator (Newport, LTA-HL) for the 1D scanning.

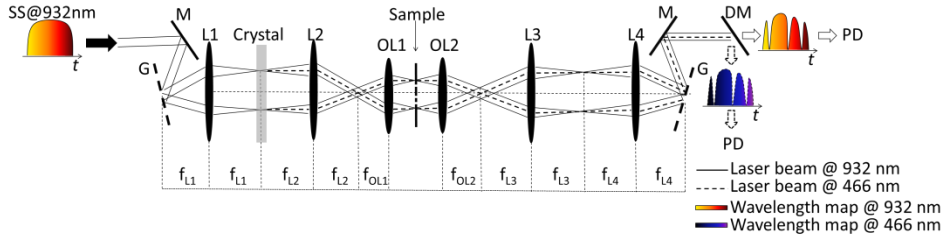

Fig. 4. The schematic diagram of the ultrafast dual-color imaging system. SS: swept source; M: mirror; G: grating; L: lens; OL: objective lens; DM: dichroic mirror; PD: photodiode.

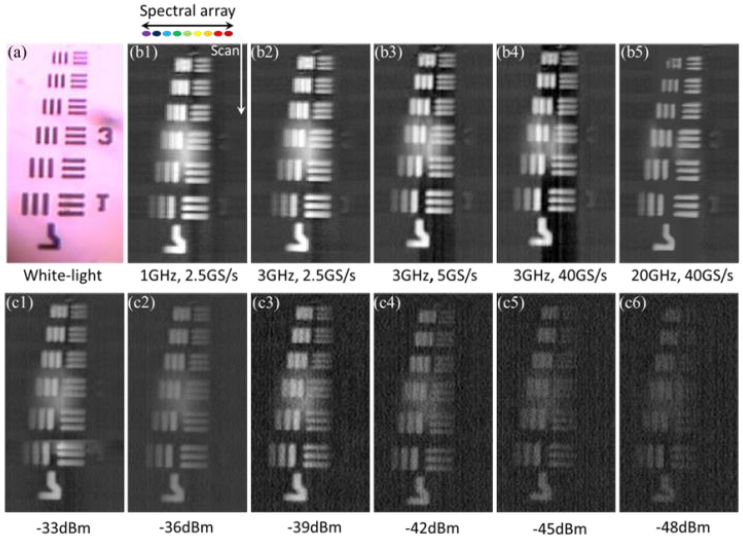

Fig. 5. The images of the USAF-1951 resolution target captured by a traditional white-light microscopy (a) and our single-shot time-stretch microscopy at 932 nm (b). Different analog bandwidths and sampling rates were set for the real-time oscilloscope. The single-shot time-stretch microscopic image was performed from top to down with a horizontal spectral array. (c) The images captured by the single-shot time-stretch imaging system with different optical powers at the PD.

At a MHz line-scan rate, i.e., 7.6 MHz in this case, the extremely-high data rate is always a concern [22], and thus the real-time data processing is the bottleneck of the ultrafast diagnosis. In most previous works [6–9], the time-stretch signal has usually been recorded by >10-GHz real-time oscilloscopes, which can easily generate a data stream of >50 GS/s. Such a heavy data processing is very difficult for the state-of-the-art electrical processors, e.g., the parallel-configured field-programmable gate array (FPGA) [23]. As a consequence, it is pressingly required to reduce the data stream without compromising the effective imaging speed. Here, we illustrate that, benefiting from this new HDF, the MHz single-shot time-stretch imaging system at 932 nm can operate at a sampling rate of only 5 GS/s, and obtain a diffraction-limited resolution. This makes it become suitable for the real-time data processing

Biomedical Optics EXPRESS

through the off-the-shelf FPGAs [23]. Figure 5(b) shows the images of an USFA-1951 resolution target captured by our time-stretch imaging system at different analog bandwidths and sampling rates. For a 20× objective lens (0.4 NA, 9 mm focal length), the spatial resolution of time-stretch imaging is theoretically calculated to be 3.5 μm, incorporating limitations from both the diffraction grating and objective lens. The spatial resolution was measured to be better than 4.3 μm, i.e., a resolving power of element 6 in group 7, as shown in Fig. 5. Consequently, a sampling rate of 5 GS/s is sufficient for current time-stretch imaging system at 932 nm, which is almost ten times slower than the previous demonstrations [24]. The field of view (FOV) was measured to be ~190 μm, while a larger FOV can also be achieved by using a wider optical spectrum. Actually, we have also performed time-stretch imaging with the conventional dispersive fiber, i.e., Nufern 1060-xp used in [24], and found it could not resolve the group 7 at the same sampling rate, i.e., 5 GS/s.

More importantly, ultrahigh imaging speed should also be realized on the basis of high sensitivity, otherwise it can be compromised by the trade-off between speed and sensitivity. In the previous demonstrations, the optical detection was usually performed with large electrical bandwidths (typically >10 GHz), which can result in a poor sensitivity due to the roll-off at high frequency. Although it can be improved by simply increasing the dispersion at the telecommunication window [9], it is not the case at the bio-favorable window, where efficient dispersive fiber has not been available before. With this new HDF, the current time-stretch imaging system at 932 nm can operate at a very high sensitivity. Figure 5(c) shows the images of resolution target captured with a decreasing average signal power in a step of 3 dB. As can be observed, an optical signal power of –48 dBm can still be detected in this new time-stretch microscopy. Considering a full power of 18 dBm and system loss of 4 dB, a sensitivity of 62 dB is obtained for this new time-stretch imaging system. Thus, it not only slows down the data stream, but also provides a very high sensitivity. Actually, an even higher sensitivity can be obtained by using extra optical amplifiers right before the optical detection, which usually can provide an additional improvement of 20-30 dB [6].

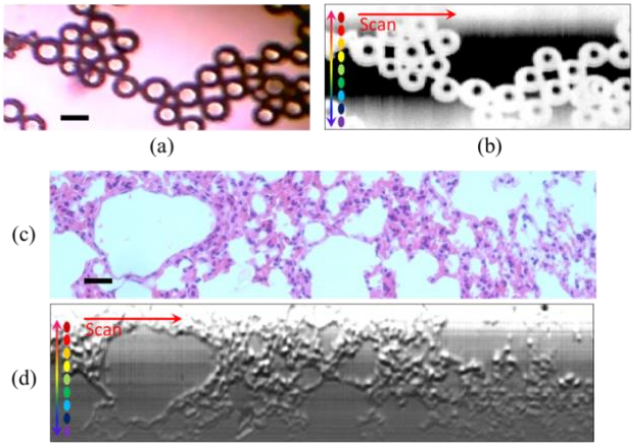

Fig. 6. The images of microspheres and H&E-stained lung tissue captured by white-light (a) and (c) and time-stretch imager at 932 nm (b) and (d), respectively. The scale bar is 50 μm.

We also captured images of some other samples using current single-shot time-stretch imaging system, as shown in Fig. 6. The glass microspheres were first dispersed in the purified water, and then transferred to a cover slide for drying at room temperature. The size of glass microspheres is ranged from 30 to 50 μm. Figure 6(a) was captured by an in-line white-light video camera (not shown in Fig. 4). In Fig. 6(b), the sample was vertically illuminated by the spectral array and horizontally scanned. It should be pointed out that epi-

Biomedical Optics EXPRESS

detection was used for the white-light camera. Bright and dark centers of the microspheres are respectively presented for white-light and time-stretch images because of the high reflection at the center with normal incidence. The lung tissue was stained with Hematoxylin and Eosin (H&E). It is clear that the cell nucleus of the lung tissue can be well manifested. The non-uniform background of images captured by the time-stretch microscopy can be attributed to three facts: the structure of optical spectrum, the polarization-dependent diffraction of grating and the uneven transmittance/reflection of specimen. It can be improved by data post-processing, e.g., subtracting the mean background.

Finally, we examined the time-stretch imaging at 466 nm. The optical spectrum of the SHG signal was captured by a miniature fiber-optic spectrometer, i.e., Ocean Optics USB2000 + , as shown in Fig. 7(a). The center wavelength is ~466 nm at a 3-dB bandwidth of 2.2 nm. Since the nonlinear crystal used in this proof-of-concept study was very thin (~30 μm), the blue-light signal after the SHG was only μW level. In addition, there is no suitable high-speed photodetector currently available in our labs for this wavelength window. Thus, we used the same spectrometer to perform spectrally-encoded imaging via a customized Matlab code for the 466-nm window. As illustrated in Fig. 7(b), since the spectrometer has a poor spectral resolution of ~0.7 nm, the spatial resolution of time-stretch imaging at 466 nm is very limited, i.e., about 20 μm in this case. In the future, several efforts can be made to realize practical time-stretch imaging at 466 nm with a higher resolution: 1) the optical power at 466 nm can be easily increased by optimizing the pump absorption and signal gain coefficient of the W-type NDF; 2) the thickness of the nonlinear crystal can be increased to obtain a higher conversion power; 3) the time-domain single-shot optical detection can be accomplished with GHz photodetectors particularly designed for the visible wavelength window, e.g., silicon photodetector and even photomultiplier tubes (PMTs) for a much higher sensitivity.

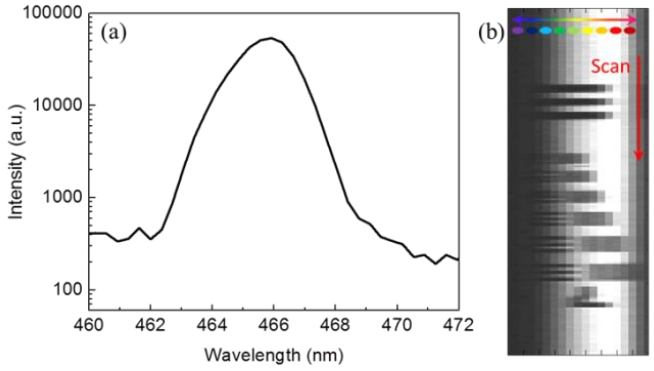

Fig. 7. (a) The optical spectrum of the SHG signal. (b) The image of the USAF resolution target captured at 466 nm.

4. Conclusion

In conclusion, we have demonstrated an ultrafast single-shot time-stretch optical imaging at a shorter wavelength window through fiber-optic engineering. It is the first time that MHz optical imaging is realized at a bio-favorable wavelength of <1000 nm with a lower data rate. The in-line frequency conversion, in addition, can enable MHz optical imaging at an even shorter wavelength window (i.e., around 500 nm), where a minimum bio-sample absorption is expected. Furthermore, a very high sensitivity of >62 dB has been identified with an angular-dispersion-limited resolution, while another 30-dB enhancement can be obtained by using extra optical amplifiers right before the optical detection. We believe that the efforts made

Biomedical Optics EXPRESS

here will ensure the ultrafast optical diagnosis at the bio-friendly wavelength window in a low-data-rate manner.

Funding

This research was supported by Research Grants Council of HKSAR, China (HKU 17208414 E and HKU 17205215), Innovation and Technology Fund (GHP/050/14GD) and University Development Fund of HKU.

Acknowledgments

Authors would like to acknowledge OFS for providing this highly-dispersive low-loss HDF.